Rare Metal Materials and Engineering
Volume 51, Issue 7, July 2022
Available online at www.rmme.ac.cn

Science Press

Cite this article as: Ma Yunzhu, Wang Jianning, Liu Wensheng, et al. Characterization of Diffusion Bonded W/Steel Joint by Electroplating-Assisted Hot Isostatic Pressing[J]. Rare Metal Materials and Engineering, 2022, 51(07): 2393-2399.

ARTICLE

Characterization of Diffusion Bonded W/Steel Joint by Electroplating-Assisted Hot Isostatic Pressing

Ma Yunzhu[1], Wang Jianning[1], Liu Wensheng[1], Dai Zhengfei[2], Cai Qingshan[1,2]

[1] National Key Laboratory of Science and Technology on High-Strength Structural Materials, Central South University, Changsha 410083, China; [2] State Key Laboratory for Mechanical Behavior of Materials, Xi'an Jiaotong University, Xi'an 710049, China

Abstract: The Ni coating of 10 μm in thickness was firstly deposited on the cylinder surface of pure tungsten by electrochemical deposition, and then the W/steel joint cylinders were prepared by the hot isostatic pressing (HIP) diffusion bonding process for nuclear component application. The HIP bonding parameters were set as 900 °C/100 MPa/1 h. The structure and composition analyses show that the metallurgical bonds are achieved with a tensile strength of about 236 MPa. However, the W/steel joint fractures at W substrate near the bonding interface due to the residual stress concentration. The Cu addition was used as the soft intermediate layer to release the residual stress by creep or yield mechanism, thereby improving the tensile strength of W/steel joint to about 312 MPa. The adhesive force of coating and the hardness distribution in the bonding interfaces were also discussed.

Key words: tungsten; steel; electroplating; diffusion bonding; hot isostatic pressing

Tungsten (W) is regarded as a promising armor material for divertor application, because of its great thermal stability, high sputtering resistance, and low tritium retention[1,2]. According to the current divertor design for demonstration reactor, the W addition into the ferritic-martensitic steel with reduced activation is commonly used as the plasma facing component[3,4]. The diffusion bonding is an attractive method to bond W with steel, due to its suitable bonding temperature and high operating temperature[5-7]. As for the W/steel fusion system, in order to avoid the grain coarsening and phase transition in steel, the joining temperature should be controlled below 1050 °C[6]. The optimal temperature for diffusion bonding of W in vacuum is about $0.67T_m$ (2200 °C)[7], suggesting that the bonding temperature of 1050 °C is too low for the W diffusion, i.e., the vacancy diffusion of W is not activated yet[8].

To improve the mechanical properties of diffusion-bonded W/steel joint, the common method is to deposit active interlayer between W and steel[9,10]. In this research, an electroplating-assisted hot isostatic pressing (HIP) method was proposed to improve the properties of W/steel joints. Firstly, the Ni plating layer was deposited on the pure W rod through electrochemical deposition technique. Then the electroplated W rod was diffusion-bonded with the circular sleeve steel by HIP method. Additionally, in order to reduce the residual stresses induced during the diffusion bonding by the large mismatch of the coefficients of thermal expansion (CTEs, 4.5×10^{-6} K^{-1} for W and $12\sim14\times10^{-6}$ K^{-1} for steel at room temperature), the Cu sheet was introduced as an interlayer. It is reported that the addition of soft Cu interlayer is an effective method to release residual stress in W/steel joint[11]. In addition, Cu can form continuous solid solution with Ni and does not form brittle phases with steel[12,13], which is attractive as an inserted material between the Ni plating layer and steel substrate.

This research demonstrates the fabrication feasibility of W/steel cylinder joint by electroplating-assisted HIP method. The interface microstructure and strength properties of the joints were also investigated.

1 Experiment

In this study, the commercially available W (99.95wt% purity, Xiamen Tungsten) and high-Cr ferritic steel (Fe-17Cr-0.1C, China TISCO) were used as parent materials. The W

Received date: July 07, 2021
Foundation item: Sponsored by State Key Laboratory for Mechanical Behavior of Materials (20202214); National Natural Science Foundation of China (51931012)
Corresponding author: Dai Zhengfei, Ph. D., Professor, State Key Laboratory for Mechanical Behavior of Materials, Xi'an Jiaotong University, Xi'an 710049, P. R. China, Tel: 0086-29-82668610, E-mail: sensdai@mail.xjtu.edu.cn

rods with dimension of Φ30 mm×50 mm (length) and the circular sleeve steel with inner diameter of 31 mm, outer diameter of 50 mm, and length of 50 mm were used for diffusion bonding. The joining surfaces of the W rods and circular sleeve steel were polished by grinding machining until the surface roughness R_a was about 1.2 μm. Both W rods and circular sleeve steel were cleaned in ultrasonic bath pot for about 10 min to remove the contaminators on surfaces before electroplating-assisted HIP experiment.

Based on electrochemical deposition technique, a Ni layer of 10 μm in thickness was deposited on the W rod surface (Fig.1). The adhesive force of the Ni coating was examined by a nano-hardness tester (VNHT, CSM Instruments) with a crosshead speed of 3 mm/min. The load range was 0~100 N, the length of scratch was 3 mm, and the diamond indenter with a tip radius of 0.1 mm was used.

For HIP diffusion bonding of the electroplated W rods with the circular sleeve steel, the Cu sheet of 99.95wt% purity and 0.5 mm in thickness was used as the inserted layer. The W and steel pieces with and without Cu interlayer were vertically placed and assembled in the 304 stainless steel canisters. Fig.2 presents the combined structure of W/steel and W/Cu/steel specimens. After gas exhaustion in vacuum chamber at 450 °C for 3 h, the pressure was less than 10^{-3} Pa. The HIP diffusion bonding experiment was conducted under the pressure of 100 MPa at 900 °C for 1 h. Subsequently, the canisters were cooled down to 400 °C at a cooling speed of 5 °C/min, and then furnace-cooled to room temperature.

The bonded specimens were sectioned into small specimens for microstructure and mechanical properties (hardness and tensile strength) investigations. The specimens for microstructure observation were prepared by standard polishing techniques. The microstructures were observed by scanning electron microscope (SEM, Novatm Nano SEM230) to investigate the diffusion zone structure. The element distribution of the bonded region was investigated by the electron probe micro-analysis (EPMA, JXA-8230F). Tensile properties of the transition joints were evaluated by a universal tensile testing machine (Instron-3369) using the specimen of 25 mm×

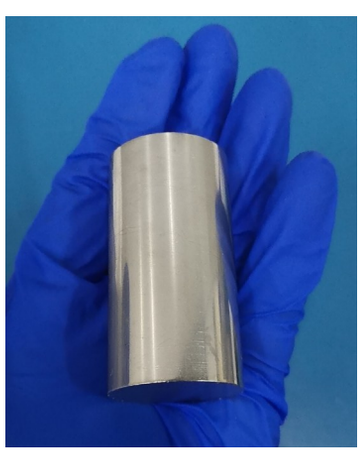

Fig.1 Appearance of Ni-coated W rod

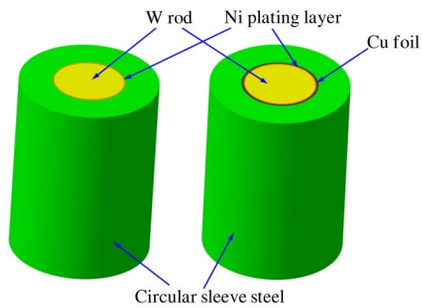

Fig.2 Schematic diagram of W/steel and W/Cu/steel specimens after assembly for HIP

8.0 mm×3.0 mm at a crosshead speed of 1 mm/min. The bonding seam was at the center of the gauge length. The fracture surfaces of the specimens were observed by SEM coupled with energy dispersive spectroscope (EDS) in secondary electron (SE) mode to reveal the characteristics and location of failure under loading. The hardness across the bonding interface was determined by the nanoindentation tester with a load of 5 mN.

2 Results and Discussion

2.1 Electroplating for W/steel joint

2.1.1 Microstructure

Fig. 1 shows that the Ni coating deposited on W rod is homogeneous and well adhered to the substrate. SEM image of the transition zone between W substrate and Ni plating layer is shown in Fig. 3a. The Ni plating layer is very homogeneous and dense, indicating a well-bonded morphology. The diffusion zone is free from cracks or discontinuities, and the bond line can be clearly observed. Fig. 3b shows EPMA element concentration curves along the red line in Fig. 3a. The diffusion traces of Ni and W elements can be observed, suggesting that Ni migrates into the W substrate and W atoms penetrates the Ni plating layer. According to the Ni-W binary phase diagram[14], Ni has extremely low solubility in W (0.3wt% at 1495 °C). The EPMA result is consistent with the Ni-W binary phase diagram.

2.1.2 Adhesive force

In order to determine the adhesive force between the Ni coating and the W substrate, the scratch tests were conducted on the coating surface. Fig. 4a shows the acoustic emission spectra of Ni-coated W rod. When the scratch length is over 1.1 mm, the acoustic emission signals suddenly increase, which corresponds to the breakdown point of the Ni coating.

When the Ni coating is scratched by the diamond indenter, the friction coefficient changes significantly. The abrupt point of the friction state is the failure point of the coating. The friction force-normal force curve of Ni-coated W rod during scratch test is shown in Fig.4b. When the normal load is about 36.67 N, there is a sudden change in the frictional force, indicating the critical load of the coating.

The adhesive force of the coating can be expressed by the

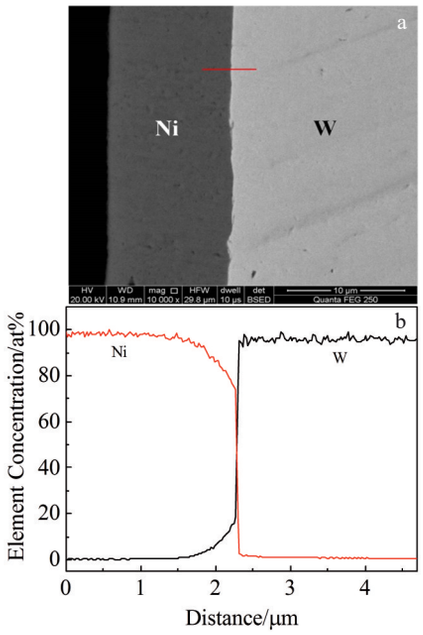

Fig.3 SEM image (a) and EPMA element concentration curves (b) along the red line in Fig. 3a (transition zone between W substrate and Ni plating layer)

critical shear stress f_s required for the stripping of the coating per unit area from the substrate, as follows:

$$f_s=[W/(\pi rp-W)]^{1/2}p \quad (1)$$

where r is the curvature radius of the tip of the diamond indenter, p is the reaction force of W matrix at length of 1.1 mm (the failure point of the coating), and W is the vertical load when the Ni coating is peeled off from the W matrix. The relationship between p and the scratch width d is as follows:

$$d=2a=(W/\pi p)^{1/2} \quad (2)$$

where a is the half width of scratch at the destruction point. The scratch width d at the destruction point (L) of the Ni coating is measured as d=10.23 μm. Substituting d and W into Eq. (1) and Eq. (2), the adhesive force can be obtained as 114 MPa. When the normal load <36.67 N, there are no transverse cracks in the scratches and no coating stripping. When the normal load ≥36.67 N, the Ni coating is peeled off from the W matrix.

2.2 HIP bonding of W and steel with and without Cu interlayer

2.2.1 Microstructure

Fig.5a shows SEM image of the W/steel joint after HIP. No unbounded regions or micro-cracks can be found along the bond zone at the W/steel joint. It should be noted that the micro-voids can be clearly seen in the Ni/steel diffusion zone. This phenomenon is related to the following facts: (1) the intrinsic diffusion coefficient of Fe ($D_{\alpha\text{-Fe}}=5\times10^{-15}$ $m^2\cdot s^{-1}$ at 900 °C) is greater than that of Ni ($D_{Ni}=3\times10^{-17}$ $m^2\cdot s^{-1}$ at 900 °C); (2) the atomic radius of Fe is larger than that of Ni; (3) the diffusivity of Ni in Fe should be larger than that of Fe in Ni. These facts produce a flux imbalance across the interface, thereby generating micro-voids. The same trend of Kirkendall void creation in diffusion-bonded interfaces in other similar materials is reported in Ref. [15, 16]. Fig. 5b shows EPMA element concentration curves across the joint interface. The diffusion traces of Fe, Cr, Ni, and W elements reveal that it is feasible to obtain a metallurgical-bonded interface of W and steel by the electroplating-assisted diffusion technique.

Fig.6 shows EPMA analysis results of element distributions of W/steel joint. According to the Ni distribution, the bonded joint contains five regions: the steel matrix, an interdiffusion zone between the Ni plating layer and steel (layer 1), the residual Ni plating layer (layer 2), the diffusion-affected zone between the Ni plating layer and the W matrix (layer 3), and the W matrix. Layer 1 reveals the diffusion traces of element Fe, Cr, and Ni. The Fe, Cr, and Ni contents change smoothly in the diffusion zone, indicating the formation of solid solution instead of intermetallic compounds. This is consistent with the Ni-Fe and Ni-Cr phase diagrams[17]. Ni is concentrated in layer 2, suggesting that this layer is the residual Ni plating layer. In layer 3, it is noted that W atoms are diffused further in Ni than Ni atoms do in W matrix, which is consistent with the diffusion traces of Ni and W elements in Fig.5b. This feature can be explained by the higher diffusivity of W in Ni than that of Ni in W. These results are similar to the results in Ref.[5,18] that for the diffusion-bonded W/steel joints with Ni interlayer at 900 °C, the penetration depth of W in Ni is much higher than that of Ni in W and a Ni-rich solid solution is formed in the W/Ni diffusion zone.

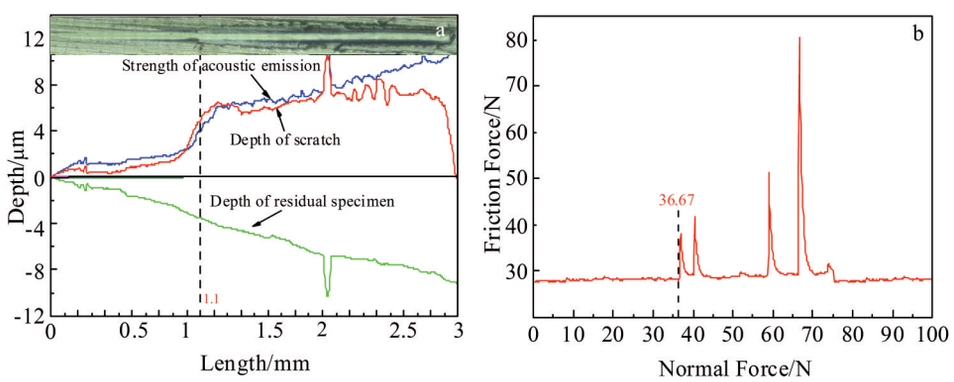

Fig.4 Acoustic emission spectra (a) and friction force-normal force curve (b) of Ni-coated W rod

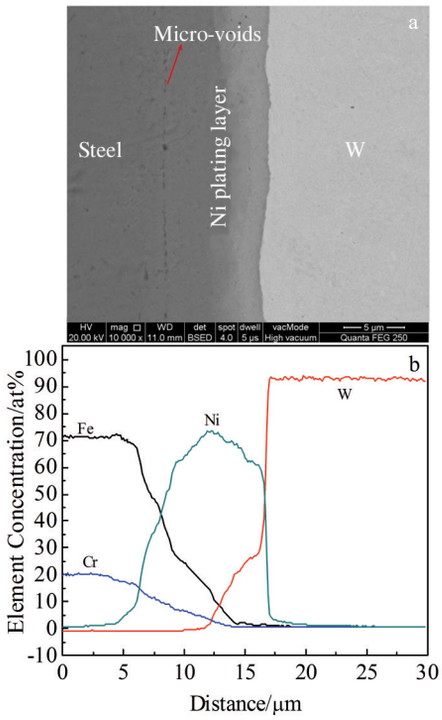

Fig.5 SEM image of W/steel joint (a); EPMA element concentration curves across the bonding interface of W/steel joint (b)

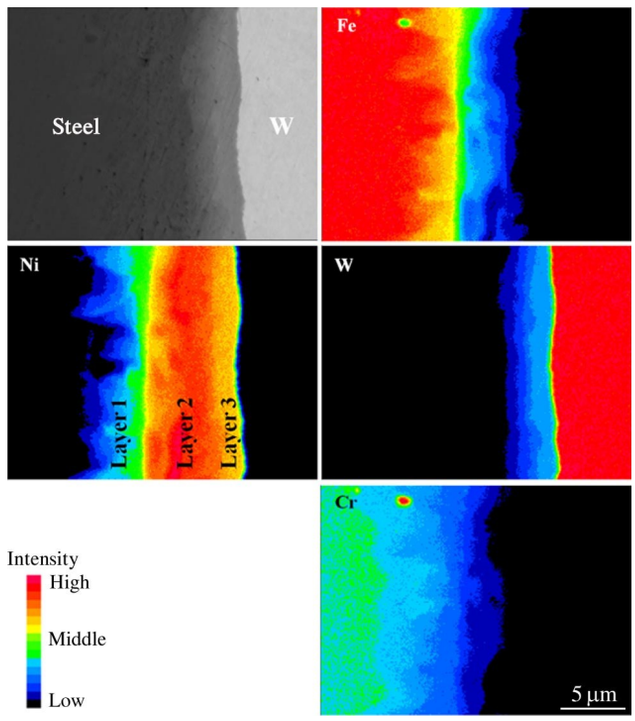

Fig.6 EPMA analysis results of Fe, Ni, W, and Cr element distributions in diffusion zone of W/steel joint

Fig.7a shows SEM image of the W/Cu/steel joint after HIP. The diffusion zone is free of cracks or discontinuities and the bond line is clear. As shown in Fig.7b, at the W/Cu interface, a smooth good interdiffusion occurs in diffusion zone, and no cracks or intermetallic compounds appear.

According to EPMA analysis (Fig. 8), several diffusion layers are formed and the thick interdiffusion zone of Ni/Cu can be observed, compared with the diffusion zone of W/Ni. This may be attributed to the enhanced interdiffusion between Ni and Cu and the low self-diffusion coefficient of W. As for the Cu/steel interface, the EPMA element content curves of Cu, Fe, and Cr clearly show smooth variation, as shown in the inset in Fig. 7c, indicating the formation of solid solution instead of intermetallic compounds. This is consistent with the Cu-Fe and Cu-Cr phase diagrams, which exhibits a good compatibility for both Cu and Fe and Cu and Cr[17].

2.2.2 Tensile strength

The tensile strength of the bonded specimens with and without Cu interlayer is ~312 and ~236 MPa, respectively. Fig.9 shows SEM fracture surfaces of the W/steel and W/Cu/steel joints. For the W/steel joint, the typical fractured surface (Fig. 9a) exhibits that the joint fails (at W side) in the intergranular mode. Due to the dissimilarity of W and steel, based on Ref. [11, 19, 20], the residual stress is formed in the bonding process caused by CTE mismatch between W and steel. In addition, the maximum residual stress is adjacent to the bonding interface at the W substrate, which is the weak region against the mechanical load[5,21]. Therefore, it is found that the W/steel joint fractures near the joint interface at W side.

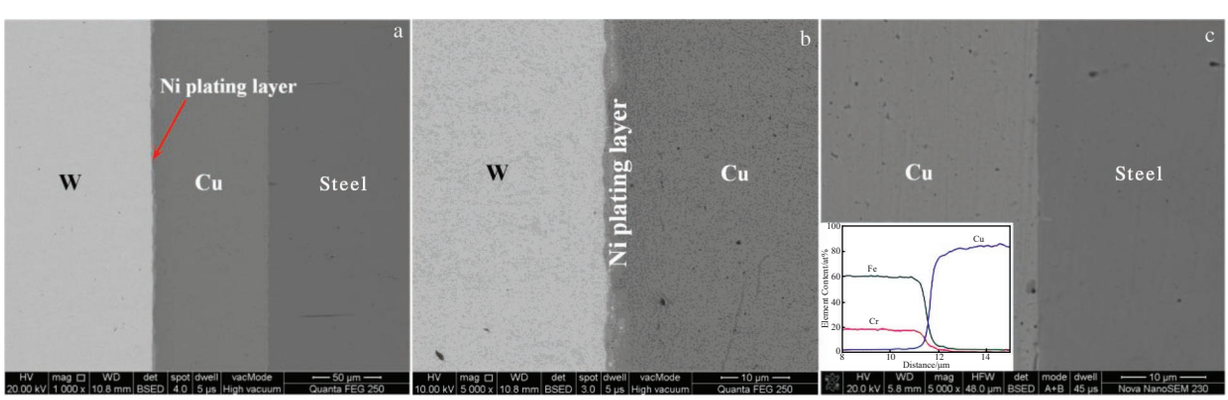

Fig.7 SEM image of cross section of W/Cu/steel joints (a); magnified images at W/Cu (b) and Cu/steel (c) interfaces with element distributions

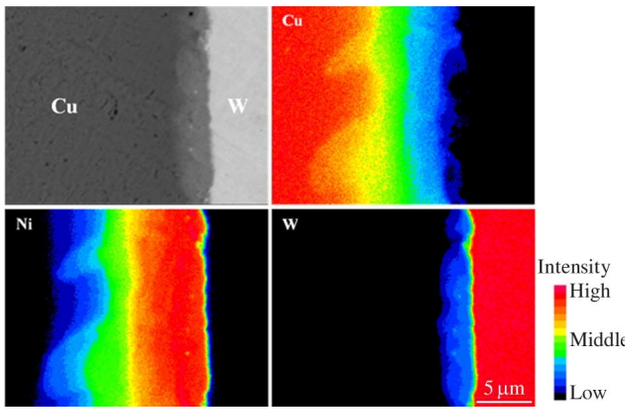

Fig.8 EPMA analysis results of Cu, Ni, and W element distributions in diffusion zone of W/Cu interface

As for the W/Cu/steel joint, the fracture surface is shown in Fig.9b and two distinct regions can be observed. As shown in Fig. 9c, the polycrystalline microstructures with some fragments appear, which is similar to the fractographs of the W/steel joint. It is deduced that the W side near the W/Cu interface is subjected to large residual stress. Fig.9d shows the typical fractured surface. The phases in region II contain W and Ni, as indicated by EDS spectrum in Fig. 9d. Compared with the microstructures of the cross-section of W/Cu/steel joint in Fig. 7 and Fig. 8, it can be inferred that region II corresponds to the diffusion zone between W and Ni. Therefore, the failure behavior of the W/Cu/steel joint during tensile tests can be explicated by the crack initiation in W matrix near the W/Ni/Cu bonding interfaces due to the residual stress concentration, and the rapid propagation along the W grain boundaries and in the diffusion zone between W and Ni plating layer.

The improved tensile strength (312 MPa) can be attributed to the reduction in residual stresses by Cu interlayer. The use of Cu interlayer with low yield strength can release the residual stress in W/steel joint by creep or yield mechanism[11,22,23], which is a very effective method to improve the strength. This is also consistent with the experiment results.

2.2.3 Nano-hardness

Fig. 10 shows the nano-hardness of W/steel joint with and without Cu interlayer. The substantial changes in hardness correspond to the interface microstructure changes. At the joint zone in W/steel joint, the hardness decreases firstly, then increases, and finally decreases (Fig. 10a). The minimum hardness of ~2.4 GPa is associated with the residual Ni plating layer. The hardness of ~5.4 GPa in the diffusion-affected zone between the Ni plating layer and the W matrix (layer 3 in Fig. 6) is associated with the migration of W into Ni plating layer. In the interdiffusion zone between the Ni plating layer and steel (layer 1 in Fig.6), a high hardness is achieved, which is caused by the penetration of Fe and Cr into the Ni plating layer and the Ni penetration into steel. The hardness variation in different zones is ascribed to the solid solution hardening effect, which is related to the interdiffusion process.

As for the W/Cu/steel joint, the hardness variation in W/Cu

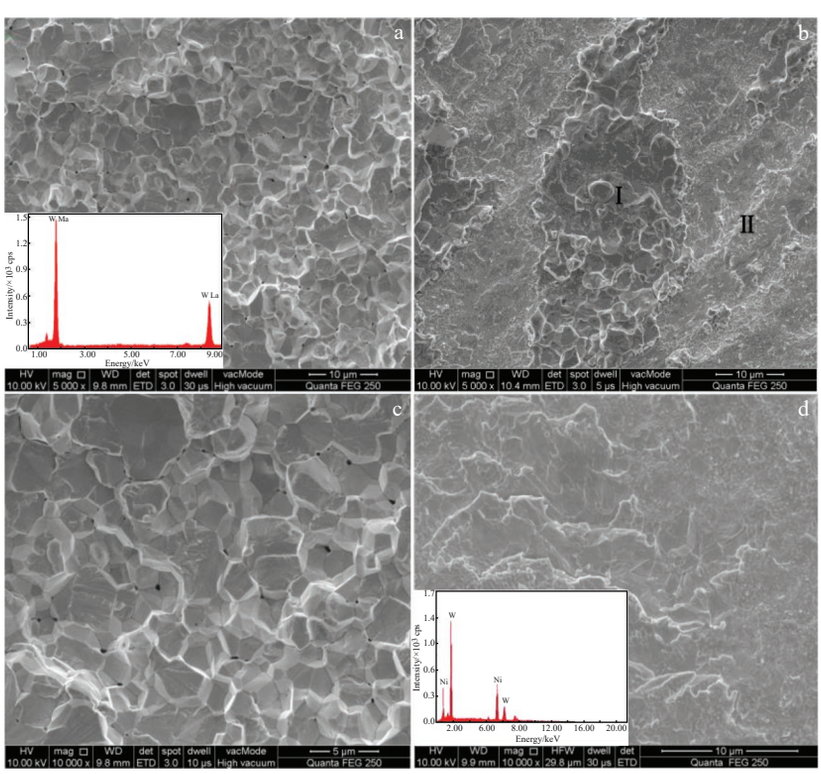

Fig.9 SEM fracture surfaces on W side and EDS spectrum of W/steel (a); morphology of W/Cu/steel (b) joints; magnified morphology of region I (c) and magnified morphology and EDS spectrum of region II (d) in Fig.9b

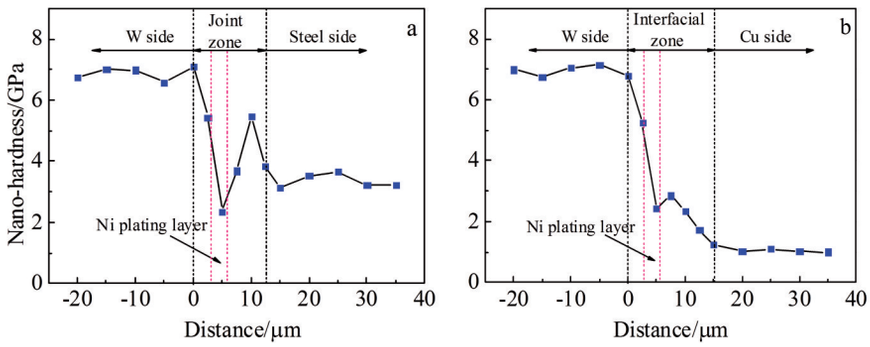

Fig.10 Nano-hardness distributions of W/steel (a) and W/Cu/steel (b) joints

interfacial zone (Fig. 10b) is similar to that of W/steel joint zone (Fig. 10a). It should be noted that, compared with the interdiffusion zone between the Ni plating layer and steel, the diffusion layer of Cu/steel interface is thicker. This is because the intrinsic diffusion coefficient of Cu (D_{Cu}=5×10^{-14} m^2 · s^{-1} at 900 °C) is greater than that of Ni (D_{Ni}=3×10^{-17} m^2 · s^{-1} at 900 °C) [16]. In particular, the low hardness of ~1.1 GPa is obtained for Cu, which is beneficial for the reduction of residual stress in the W/Cu/steel joint by the creep or yield mechanism[11].

3 Conclusions

1) The Ni-coated W/steel joints can be prepared by hot isostatic pressing coupled with diffusion bonding method. No cracks or interfacial defects can be observed in the joints.

2) No intermetallic compound is formed at the joint interfaces. The tensile strength of the W/steel joint is ~236 MPa. All the joints fracture in the brittle fracture mode near the bonding interface at W side, resulting from the residual stress concentration in the joints.

3) The Cu interlayer can be used to release stress in the diffusion bonding between W and steel. The strength of the W/Cu/steel joint is ~312 MPa, and the joints fracture at W substrate and the diffusion zone between W and the Ni plating layer.

References

1 Philipps V. *Journal of Nuclear Materials*[J], 2011, 415(1): 2
2 Zhou Wuping, Wang Ling, Qin Yingnan *et al. Rare Metal Materials and Engineering*[J], 2020, 49(11): 3957
3 Norajitra P, Giniyatulin R, Ihli T *et al. Fusion Engineering and Design*[J], 2007, 82(15-24): 2740
4 Hu Ke, Yang Shisong, Zou Liming *et al. Rare Metal Materials and Engineering*[J], 2020, 49(10): 3472
5 Zhong Zhihong, Jung Hunchea, Hinoki Tatsuya *et al. Journal of Materials Processing Technology*[J], 2010, 13(210): 1805
6 Basuki W W, Aktaa J. *Fusion Engineering and Design*[J], 2011, 86(9-11): 2585
7 Oono Naoko, Noh Sanghoon, Iwata Noriyuki *et al. Journal of Nuclear Materials*[J], 2011, 417(1-3): 253
8 Basuki W W, Aktaa J. *Journal of Nuclear Materials*[J], 2011, 417(1-3): 524
9 Cai Qingshan, Liu Wensheng, Zhao Zhongwei *et al. Fusion Engineering and Design*[J], 2017, 125: 189
10 Krauss Wolfgang, Lorenz Julia, Holstein Nils *et al. Fusion Engineering and Design*[J], 2011, 86(9-11): 1607
11 Cai Qingshan, Zhu Wentan, Ma Yunzhu *et al. International Journal of Refractory Metals and Hard Materials*[J], 2018, 70: 155
12 Elrefaey A, Tillmann W. *Journal of Materials Processing Technology*[J], 2009, 209(5): 2746
13 Zhang Jiajia, Xie Donghua, Li Qishou *et al*. *Materials Letters*[J], 2020, 261: 1268
14 Tian Haixia, Lin Chaoying, Shi Chenying *et al. Nb-Ni-W Ternary Phase Diagram Evaluation*[R]. Stuttgart: MSIT, 2016
15 Zhou Xiaosheng, Dong Yutao, Liu Chenxi *et al. Materials and Design*[J], 2015, 88: 1321
16 Sabetghadama H, Hanzakia A Z, Araee A. *Materials Characterization*[J], 2010, 61(6): 626
17 Nayeb H A A, Clark J B. *Binary Alloy Phase Diagrams*[M]. Geauga: ASM International, 1991
18 Zhong Zhihong, Hinoki Tatsuya, Kohyama Akira. *Materials Science and Engineering A*[J], 2009, 518(1-2): 167
19 Liu Wensheng, Sheng Qingqing, Ma Yunzhu *et al. Fusion Engineering and Design*[J], 2020, 156: 111 602
20 Cai Qingshan, Liu Wensheng, Ma Yunzhu *et al. International Journal of Refractory Metals and Hard Materials*[J], 2015, 48: 312
21 Kalin B A, Fedotov V T, Sevrjukov O N *et al. Journal of Nuclear Materials*[J], 2004, 329(B): 1544
22 Zhou Yunhong, Ikeuchi Kenji, North T H *et al. Metallurgical Transactions A*[J], 1991, 22(11): 2822
23 Travessa Dilermando, Ferrante Maurizio, Ouden Gertden. *Materials Science and Engineering A*[J], 2002, 337(1-2): 287

电镀辅助热等静压扩散连接钨/钢接头的特征

马运柱[1]，王健宁[1]，刘文胜[1]，戴正飞[2]，蔡青山[1,2]
(1. 中南大学 轻质高强结构材料国家级重点实验室，湖南 长沙 410083)
(2. 西安交通大学 金属材料强度国家重点实验室，陕西 西安 710049)

摘　要：采用电化学沉积技术在纯钨圆柱表面上电镀了厚度为10 μm的Ni镀层，再利用热等静压扩散连接方法制备可应用于核聚变堆部件的钨/钢圆柱体连接试样。热等静压扩散连接工艺参数设定为900 ℃/100 MPa/1 h。由组织和成分分析可知钨/钢扩散连接接头形成了良好的冶金结合，其接头抗拉伸强度约为236 MPa，但由于残余应力集中，钨/钢接头断裂失效发生在靠近连接界面的钨基体内。实验加入Cu作为软质中间层，通过蠕变或者屈服机制释放残余应力，使得钨/钢接头强度提高到312 MPa。同时分析了镀层的结合力和钨/钢连接接头界面的硬度分布。

关键词：钨；钢；电镀；扩散连接；热等静压

作者简介：马运柱，男，1975年生，博士，教授，中南大学轻质高强结构材料国家级重点实验室，湖南 长沙 410083，E-mail：zhuzipm@csu.edu.cn